Structural Differentiation of Tooth Supporting Substances with the Electromechanical Impedance Technique

Hector A. Tinoco[1,*], Juan P. Gomez[2], Johana Torres[2], Maria A. Velasco[2]

[1]Department of Mechanics and Production, Universidad Autónoma de Manizales (UAM). Grupo de Diseño Mecánico y Desarrollo Industrial. Antigua Estación del Ferrocarril, edificio Sacatín C.P. 170001. Manizales-Caldas. Colombia.

[2]Department of Health, Universidad Autónoma de Manizales, Grupo Salud-INSAO Antigua estación del Ferrocarril, Edificio Sacatín C.P. 170001. Manizales-Caldas. Colombia.

[*]Author to whom correspondence should be addressed. Phone: Tel: +5768727211. Email: htinoco@autonoma.edu.co

***Abstract* -- In this study, an experimental method is described to identify and differentiate materials that act as constraints on a host structure, which define the boundary conditions. The main structure is composed of a tooth with a stainless steel bracket bonded to the crown, which in turn is coupled to a "smart" beam (piezoelectric materials attached) fixed to the bracket slot. The root portion of the tooth is imbedded in different supporting materials (substructures), which generate clamped conditions to the tooth. A substructure composed by piezoelectric transducers is bonded to the beam to generate vibrations to the system. The method applies high frequency vibrations (between 5-10 KHz) through the beam which in turn moves the tooth, obtaining a mechanical response from the material where it is implanted. To quantify the mechanical responses, the electrical impedance is read from piezo-transducers by means of electromechanical impedance technique (EMI). In a window observation in frequency, it was possible to identify a similar trend in the derivatives of the electrical impedance obtained for five different materials made for two teeth; molar and canine. Results suggest that the measurements are invariant to the interface (in this case, the tooth) that couples supporting substances, implying that the materials were identified, independently of the tooth.**

***Index Term* -- Structural differentiation, electromechanical impedance, smart beam, tooth, Bone density**

I. Introduction

Orthodontic treatments have helped to achieve oral rehabilitation during decades correcting anomalies in the position and growth of bone structures, by means of mechanical-biological stimulus. In orthodontic treatment, teeth are moved to better positions, a procedure that can be done in months or years, depending on final location. In the field of orthodontic, it is important to understand orthodontic tooth movement (OTM) and to comprehend the biological events that occurs in alveolar bone when mechanical forces are applied to the teeth. It has been reported that the modification of mechanical environment in bone structure produces changes in the bone density during the orthodontic treatment [1-2, 27]. Different studies have shown that alveolar bone fraction and tissue mineral density can reduce with age and during orthodontic tooth movement [29-32]. Site-dependent, anatomical characteristics of maxillary bone also determine bone density [5,28]. Recent studies have centered their efforts in understanding those changes at the cellular and molecular levels from experimental and numerical research [3-6, 27, 34-37]. It shows that bone density is a determinant parameter in the OTM process since the changes determine the treatment time, as explained in [38]. Techniques for bone density assessment include: Radiogrammetry (RG), Compton Scattering Technique; Radiographic Photodensitometry (RP); Dual-energy Photon Absorptiometry (DPA) among others [28]. In general, the majority of current techniques are considered invasive, since quantification of bone density depends on the use of ionizing radiation (X rays). Therefore, alternative methods should be explored to evaluate alterations in bone density.

Piezoelectric transducers (PT) are used in structures to monitor their physical integrity, taking advantage of electromechanical phenomenon provided by these. It is possible to evaluate, identify, classify and estimate different structural conditions with PT, as it has been proven in different engineering fields; Non-Destructive Evaluation (NDE), Structural Health Monitoring (SHM) and Control among others [7-11]. Active methods that use PT are frequently applied in these fields, in which we can observe the electromechanical impedance (EMI) technique. EMI technique has evidenced a great potential in the area of damage detection and structural condition since many applications demonstrate that the technique presents a great capacity and sensitivity of capturing structural modifications in high frequency when the signals are compared with a reference measure, such as shown by [23-26].

Recent studies have explored the application of EMI technique in the bio-medical field, such as the use of piezoelectric ceramics as biomedical sensors for monitoring condition of bones, through experimental studies on human and rabbit bones [39], where the changes in the EMI signatures correlated fairly well with the changes in the condition of the bones. Additionally, [40] applied a method that consists in putting a healing agent in particular cracks in bone to be monitored by PZT-needle sensor, which is embedded in it. The measurements

were taken in the frequency range between 0.04 to 100 kHz, at 1 kHz interval using AD5933 evaluation board. The results of the study showed feasibility to detect changes during healing process until the cracks in bone are fully recovered. Applications corresponding to structural modification assessment were extrapolated to the orthodontic field. For example, [12-13] proposed a technique for monitoring dental implant stability applying the EMI technique. The method involved bonding a piezoelectric transducer to the implant in which the electrical admittance was measured to evaluate its stability, which in turn was correlated with the mechanical parameters of the bone.

This study presents a new method based on in a *bracket-beam-piezoelectric sensor* (BBPS) to differentiate different tooth supporting substances with electromechanical impedance (EMI) technique. The proposed mechanical system designed for the experiment is composed of a tooth with a stainless steel bracket bonded to the crown and a stainless wire that acts as a beam that in turn it is fixed to the bracket slot. The tooth supporting substances simulate various bone qualities by changing the model's constituent material. An experimental procedure is applied to identify and differentiate these tooth supporting substances.

II. Materials and Methods

A. *Theoretical Background of Electromechanical impedance Technique (EMI)*

In the circuit theory, electrical impedance $Z_p(\omega)$ refers to the opposition that is encountered to the current $i(\omega)$ when a harmonic voltage $V(\omega)$ is applied on the circuit. It implies that a linear relation is kept as unique ratio between $V(\omega)$ and $i(\omega)$. An electrical circuit is a combination of electrical resistance (R), inductive reactance (X_L, L inductance) or capacitive reactance (X_c, C capacitance) as depicted in Fig. 1a. The interaction of the elements that compose the circuit depends on the combination of elements in which these are analyzed, since these elements can be analyzed at the time domain or in the frequency domain.

The electrical constants (R, L and C) act as a vector in frequency spectrum, therefore it is possible to establish an impedance triangle, as illustrated in Fig. 1b, such that ϕ is the phase and $Z_p(\omega)$ is the magnitude. Depending on the vector direction, the nature of the circuit can be observed, we distinguish inductive circuits, capacitive circuits, resistive circuits, or their combination. From this point of view, it means that intrinsic properties of the circuit do not change. Therefore, these parameters do not depend on the voltage input and the current output or vice versa. Additional information about the electrical impedance principles can be found in [14].

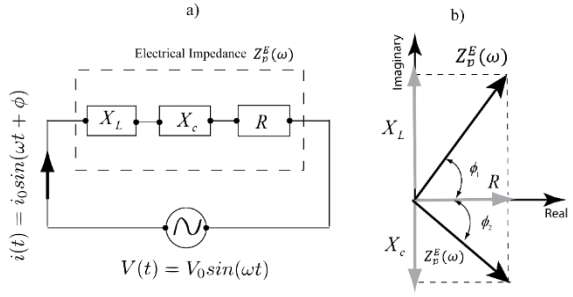

Fig. 1.. a) Series combination of LCR circuit (resistance R, inductance L and capacitance C). b) Impedance triangle for RLC circuit [10].

Piezoelectric transducers (PT) present electrical properties that are coupled to the mechanical properties by the electromechanical phenomenon. For example, when a piezo-transducer is deformed an electrical charge is produced or when an electrical field is applied on the piezo-transducer, it deforms [15]. According to [16], PT can be analyzed as an open electrical circuit or short circuit, respectively. If a piezo-transducer is connected to a circuit all the mathematical operations done in circuit theory can be performed on it. A piezo-transducer in sheet form can be represented by a combination of resistance and capacitance [17]. It means that there is no inductance in a piezo-transducer. Then, the properties of electrical circuits satisfy to the PT. We can mention to the electrical admittance $Y_P^E(\omega)$, which is the relation between current, $i(\omega)$ and voltage $V(\omega)$ that goes through it. It is recognized that $Y_P^E(\omega)$ is the inverse $Z_P^E(\omega)$. $Y_P^E(\omega)$ is composed by a real part (conductance G) and an imaginary part (susceptance B) and it may be described as

$$Y_P^E(\omega) = \frac{i_0(\omega)}{V_0(\omega)} = \frac{1}{Z_p^E(\omega)} = \frac{1}{R + Xj} = G + Bj, \quad (1)$$

where ω is the frequency. The constants inside G and B can be determined using a parameter identification from the electrical impedance. Where R is the resistance and X is the reactance which can be inductive and capacitive.

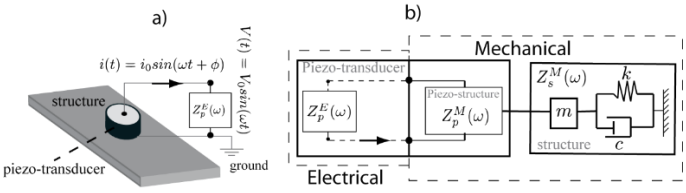

Fig. 2. a) Electromechanical scheme piezo-transducer-structure. b) Coupled electromechanical system of one degree of freedom [10,17-18].

Fig. 2a shows a simple model that couples a mechanical system with an electrical system. [17] determined electromechanical admittance of this dynamic system and they obtained a one-dimensional model of a piezo-transducer bonded to a structure as follows:

$$Y_P^E(\omega) = \frac{2\omega j w_p}{h_p}\left[e_{33} - d_{31}^2 \bar{y}^E + \left(\frac{Z_p^M(\omega)}{Z_p^M(\omega) + Z_s^M(\omega)}\right) d_{31}^2 \bar{y}^E \left(\frac{\tan(kl_p)}{kl_p}\right)\right], \quad (2)$$

where, h_p is the thickness, l_p is the length, w_p is the width of the piezoelectric sheet, d_{31} is the piezoelectric strain coefficient corresponding to $x(1)-z(3)$ coordinates, $\bar{y}^E = y^E(1+\eta)$ is the complex Young's modulus of the piezoelectric sheet, at constant electric field and $\bar{e}^\sigma = e^\sigma(1+\delta)$ is the complex electric permittivity of the piezoelectric material at constant stress. η and δ denote both mechanical loss and dielectric loss factors, k is the wave number and it is given by

$$k = \omega\sqrt{\frac{\rho}{\bar{Y}^E}}, \tag{3}$$

ρ is the density of piezoelectric material, ω is the angular frequency and $Z_p^M(\omega)$ is the mechanical impedance of the piezoelectric patch, which it can be calculated by

$$Z_P^M(\omega) = \frac{kh_p\bar{Y}^E w_p,}{j\omega\tan(kl_p)}, \tag{4}$$

A model published by [17] (See Eq. (1)) and later modified by [19] included an adhesive interface between structure and piezo-transducer; this modification was represented by a constant. However, [18] determined that the value of coupling constant depends on changes in the frequency. The simple model is widely accepted yet and the adhesive effects on the EMI are studied actually. In the structure, $Z_s^M(\omega)$ represents the mechanical impedance, which is given in terms of frequency as

$$Z_s^M(\omega) = \frac{K_s^M(\omega)}{j\omega}, \tag{5}$$

where $K_s^M(\omega)$ is the dynamic stiffness of the structure and it is describe by

$$K_s^M(\omega) = \frac{F_s(\omega)}{X_s(\omega)}, \tag{6}$$

hence, $F_s(\omega)$ is the applied force and $X_s(\omega)$ is the displacement of a driven-point on the structure. In modal analysis, the mechanical impedance of a system is represented by a matrix $Z_{sij}^M(\omega)$, which is a symmetrical matrix. It is important to acknowledge that mechanical impedance reflects the properties of a linear vibration system.

Table I

Materials for the specimens

Teeth	Material	Proportion	Curing time	Commercial house
Canine	Black silicone (Type I)	60 ml	24 hours	Sikasil®
Molar	Transparent silicone (Type II)	60 ml	24 hours	Sikasil®
Canine-Molar	Hard Rock 2 (White gypsum)	100 gr/ in powder for 40 ml of water	5-7 min	General plaster®
Canine-Molar	Hard Rock 5 (Green gypsum)	100 gr/ in powder for 40 ml of water	10 min	Whip Mix®
Canine-Molar	Transparent Acrylic	Monomer 60 ml/ polymer 60 ml	15 min	Veracril®

Therefore, they do not depend upon external forces nor displacements. The dependency may occur only if the dynamic system has a nonlinear behavior, such as friction or material dependency on frequency. A detailed description of modal analysis can be reviewed in [20].

B. *Specimens for Tooth Supporting Substances*

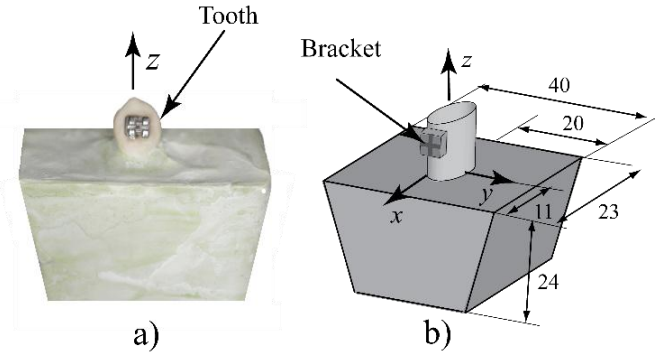

Fig. 3. Tooth supporting specimens and dimensions in mm

For the experimental tests, only two teeth (molar and canine) are chosen as main structures and these are embedded in the supporting substances; as shown in Fig. 3. For each tooth (molar and canine), five supporting substances are prepared and the materials are listed in Table 1. The materials used are; transparent Silicone – Type I (Molar), White Gypsum, Green

Gypsum, Transparent Acrylic and Black silicone-Type II (Canine). Test specimens are originally designed with 40 mm of length, 23 mm of width and 24 mm of height as depicted in Fig. 3b. The preparation was carried out on a standard mold made for this purpose. Time of preparation of each specimen is described in Table 1.

Tooth location and position is standardized using a rubber template over which the tooth is located in the center of the tooth-supporting specimen. To avoid influences of factors in the experiments; the canine and molar are embedded separately in the same supporting substances with the aim to demonstrate that the materials can be identify independently of the embedded interface, which in this case is represented by the teeth.

Subsequently, a stainless steel bracket is bonded at the center of the buccal surface of each tooth crown. The slot of the bracket serves as retaining mechanism for the beam that it will be used as sensor, as described in the next section.

C. *Experimental Setup and Bracket-Beam-Piezoelectric Sensor (BBPS) Principles*

In this study, EMI technique will be applied to evaluate tooth-supporting substances by means of an in-house designed, electro-mechanical device that contains a piezoelectric transducer, called “bracket-beam-piezoelectric sensor” (BBPS). This sensor is constructed with the intention of differentiating the material used as tooth-supporting substance with an indirect measurement, provided by the electromechanical impedance of the piezoelectric transducer.

To study the feasibility of differentiation of the tooth supporting substances, an experimental setup is proposed using a piezo-electric sensing device and a specific testing protocol applying the EMI technique. The experimental included four principal elements; 1. BBPS ; 2. tooth ; 3. supporting substance; and 4. measurement instrument (Impedance analyzer AD5933). Previously, two teeth and five supporting substances were prepared for the experiment, as explained in section 2.2.

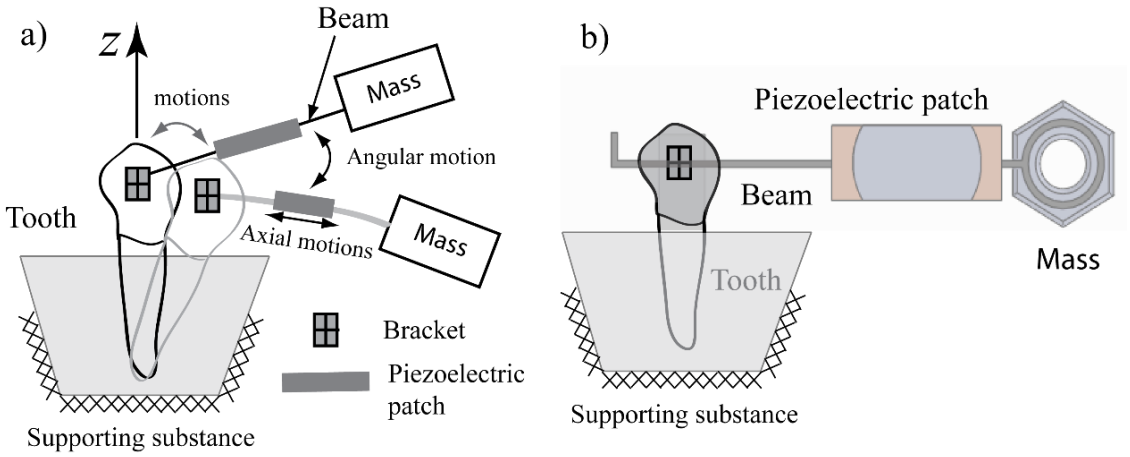

Fig. 4. a) Working principle of the BBPS. b) BBPS coupled to the tooth.

A schematic drawing of the fundamental working principle of the BBPS is shown in Fig. 4a. BBPS incorporates in the bracket slot a beam made of 0.017 x 0.025 stainless steel wire used in orthodontics treatments. Additionally, piezoelectric patches are bonded to the wire with epoxy adhesive forming a composite joint. A mass is added to complete an inertial system at the end of the beam, as shown in Fig. 4b. Piezo-transducers used in the BBPS were acquired as SEN10293ROHS (SparkFun Electronics, Niwot, CO.) [21] ,an these are shown in the experimental setup of Fig. 5.

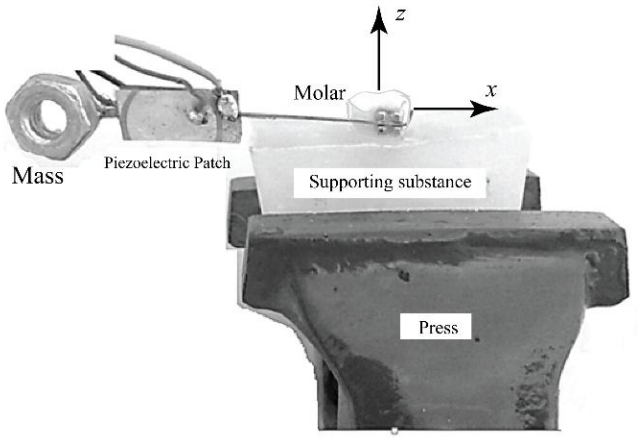

Fig. 5. Experimental setu

The experimental trial was implemented in the following sequence; BBPS was attached to a bracket bonded to a tooth crown specimen that is embedded in the supporting substance.

The objective is to move the beam-mass mechanical system by the inertia produced when the piezo-patches are activated by a harmonic electrical signal emitted from an impedance analyzer AD5933 (Analog Devices Inc., Norwood , MA.) [22]. Our assumption and working hypothesis is that the beam-mass moves the tooth, due to its bending, as consequence of piezoelectric stimulation. It is important to clarify that the experiments are designed to test that BBPS can measure the supporting substrates, regardless that the tooth is embedded in it, in this case, canine and molar. The presented methodology should validate the correlation between the supporting substrates obtained from both teeth (canine and molar). For our experiments, we used an impedance analyzer which measures the electrical impedance and phase of the signatures emitted by the BBPS. The frequency spectrum defined for the experiment is between 5 to 10 KHz, with increments of 10 Hz; this was obtained previously from an exploratory data analysis.

D. *Index J_m for comparing the impedance signals*

It is known that the electrical impedance of a piezo-transducer combines the mechanical parameters of all substructures coupled to it. In the frequency spectrum, resonance peaks appear inside electrical impedance. These corresponds to the natural frequencies that can be reflected in the electrical impedance. Let's consider an electrical impedance signal with a resonant peak which correspond to the coupled mechanical system, such as illustrated in Fig. 6. Two parameters can be observed in each resonant peak; the value of frequency ω_r and the change in the resonant peak (see the derivative in Fig. 6). Therefore, if the derivative is extracted in an observation window, we can characterize the information of the coupled structure. Based on this consideration, we propose an index to quantify the changes in the resonant peak, when the BBPS is coupled with a supporting substance, such that

$$J_m = \frac{\sqrt{2}\sigma h^2}{\int_a^b f(x)dx} 1\times 10^3 \ [\%], \qquad (7)$$

where σ is standard deviation, h is the height of a distribution function and $f(x)$ is an approximation function. To clarify the correspondence and correlation between signals obtained from each tooth, the numerical derivative $dZ(\omega)/d\omega$ should be determined for the electrical impedance. From an exploratory data analysis, we propose to approximate $dZ(\omega)/d\omega$ by a Gaussian functions which are represented in the following equation:

$$f(x) = y_0 + \frac{A}{w\sqrt{\pi/2}} e^{-\frac{(x-x_c)^2}{2w^2}}. \qquad (8)$$

where y_0, A, x_c and w are constants.

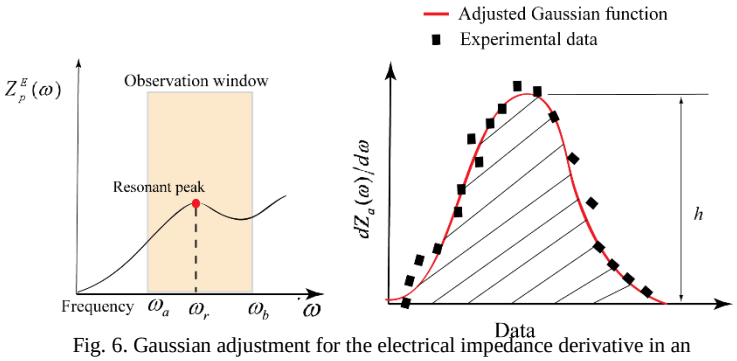

Fig. 6. Gaussian adjustment for the electrical impedance derivative in an observation window.

III. Results and Discussion

In Fig. 7a and b, four electrical impedance signals are shown, those that were taken for each supporting substances (Black silicone, transparent silicone, White gypsum, green gypsum, Transparent acrylic) with the BBPS. To carry out the experimental tests, each specimen model (see Fig. 3) was mounted in a press to simulate boundary conditions of zero displacements on x direction in the exterior surface of each supporting substance, as depicted in Fig. 5.

In figures 7a and b, similar behavior or trends are observed for each supporting substance. Initially, we can compare the signals in the range where the peaks appear; subsequently the range is estimated at 6.75 and 8.75 KHz and it is defined at 6.5 and 9.5 KHz for figures 7a and b. Those regions are demarked with yellow color boxes in the figures, when each resonance peak is located in both figures, it is evident that the White Gypsum begins in the first position followed by the Acrylic signal and the Silicon (transparent and black) signal ending in third place. Additionally, we observe that the signal for Green Gypsym does not have a resonant peak; however both signals (molar and canine) present the same behavior. For easy comprehension of the above affirmation, each peak was labeled with the same number in both figures.

It is clear in the experiment that the signals can be correlated since these present a correspondence in its shape and location. However, this should be demonstrated objectively because the main purpose of this study is to differentiate the supporting substances with a methodological procedure.

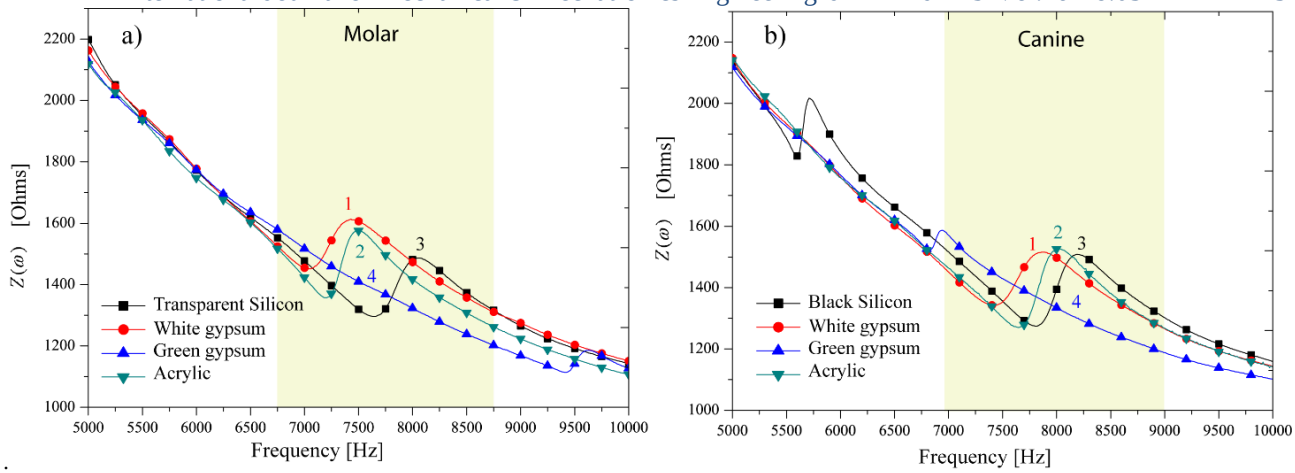

Fig. 7. Electromechanical impedance for: a) Molar tooth. b) Canine tooth.

Table II
Approximated Gaussian models

Tooth		**Molar**				**Canine**		
Coefficients	Transparent Silicone	W. Gypsum	G. Gypsum	Acrylic	Black Silicone	W. Gypsum	G. Gypsum	Acrylic
y_0	-0.318	-0.300	-0.209	-0.300	-0.302	-0.337	-0.192	-0.390
x_c	7992.819	7637.086	8777.783	7229.956	7841.835	7853.473	8828.352	7338.545
w	226.289	294.219	946.566	254.190	251.7658	202.712	865.781	171.019
A	392.01	354.281	97.384	318.075	352.190	408.138	58.539	365.634
Reduced Chi	2.53×10^{-3}	2.98×10^{-3}	0.00228	4.37×10^{-3}	2.66×10^{-3}	4.33×10^{-3}	0.32198	2.53×10^{-3}
R-Square	0.988	0.974	0.15954	0.963	0.981	0.879	0.05166	0.99
P>F ANOVA)	0	0	0	0	0	0	0	0

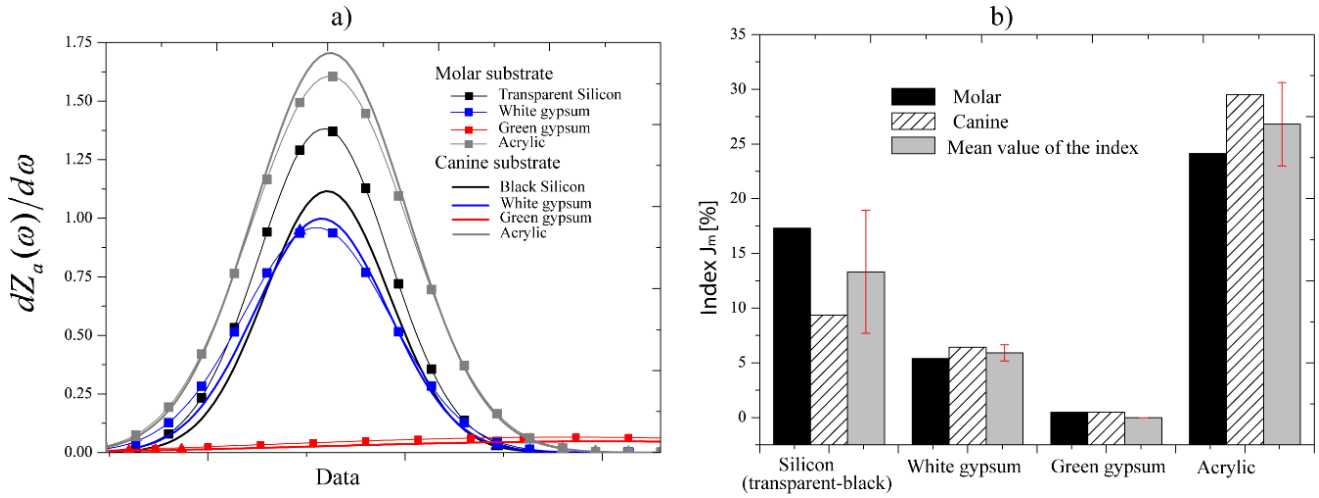

Fig. 8. a) Gaussian fits for the electrical impedance derivative. b) J_m index for different supporting substances

For the purpose of comparison, the numerical derivative is calculated for the each electrical impedance. Eight Gaussian models are approximated to the numerical derivatives using Equation (8). In Table 2, there are listed all parameters determined for the Gaussian models in which we analyze that all models are well correlated. Correlations coefficients and ANOVA show a good agreement, except data determined for Green Gypsum. The approximations are illustrated Fig. 8a. The models were normalized from the following calculation:

$$dZ_a(\omega)/d\omega) = \left|dZ(\omega)/d\omega - \min(dZ(\omega)/d\omega)\right|. \qquad (9)$$

We can observe in Fig 8a that white gypsum, green Gypsum and Acrylic present very close distributions and a good correlation is perceived among them (between canine and molar. Nonetheless, the silicone is not well correlated showing higher differences. which make sense since the type of silicone is different for each tooth; molar (transparent) and canine (black). It is important to remember that experiments were

done separately; although these conclude that the canine and the molar act as intermediate source to transmit motions between the supporting substance and BBPS. It means that the BBPS measurements are invariant to the coupling interface (for this case the tooth) which allows to transmit motion to the supporting substances. To quantify the differences in between the approximated derivative signals, J_m index is calculated and shown in Fig. 8b. With the index, each supporting substance is easily identifiable and differentiable. For example, the index for the silicone material finds in a range of 9.34-17.29 %; white gypsum 5.39-6.43 %, green gypsum 5.42-2.96 $\times 10^{-4}$ % and acrylic 24.11-29.5 %. It is observed that all supporting substances are in different ranges of measurement and these are similar in booth teeth. In Fig 8b, the mean of each supporting substance with its respective standard deviation is determined, showing the feasibility of observing the material using the BBPS. As final consideration, we see a great opportunity to correlate the J_m index with any mechanical parameter of the supporting substances.

IV. Conclusions

The present study proposed a methodology for structural differentiation of tooth supporting substances, through electromechanical impedance (EMI) measurements obtained with a sensor called BBPS. Experiments performed with BBPS showed satisfactory results, which suggest a preliminary validation of the exposed methodology. In these tests, it was possible to identify a similar trend in the EMI obtained from four substances supporting for two different teeth, a molar and a canine. Using Gaussian approximations, it was possible to correlate similar supporting substances and identify which were relatively similar applying a proposed index. The index corroborates the correlation and differentiation between supporting substances since regions were differentiated for the five materials used in the experiments.

In a clinical context, we perceived an opportunity to study bone density occurring in alveolar bone using a low cost-effective non-invasive method. However, many experimental aspects should be improved to diminish the errors induced by factors as geometrical variations of the tooth supporting substances.

References

[1] Teitelbaum, S. L. 2000. Bone resorption by osteoclasts. *Science*, *289*(5484), 1504-1508.

[2] Kiberstis, P., Smith, O., & Norman, C. 2000. Bone health in the balance. *Science*, *289*(5484), 1497-1497.

[3] Lee, M. Y., Park, J. H., Kim, S. C., Kang, K. H., Cho, J. H., Cho, J. W., .& Chae, J. M. 2016. Bone density effects on the success rate of orthodontic microimplants evaluated with cone-beam computed tomography. *American Journal of Orthodontics and Dentofacial Orthopedics*, *149*(2), 217-224.

[4] Park, H. S., Lee, Y. J., Jeong, S. H., & Kwon, T. G. 2008. Density of the alveolar and basal bones of the maxilla and the mandible. *American Journal of Orthodontics and Dentofacial Orthopedics*, *133*(1), 30-37.

[5] Park, H. S., Lee, Y. J., Jeong, S. H., & Kwon, T. G. 2008. Density of the alveolar and basal bones of the maxilla and the mandible. *American Journal of Orthodontics and Dentofacial Orthopedics*, *133*(1), 30-37.

[6] Gomez, J. P., Peña, F. M., Martínez, V., Giraldo, D. C., & Cardona, C. I. 2014. Initial force systems during bodily tooth movement with plastic aligners and composite attachments: A three-dimensional finite element analysis. *The Angle Orthodontist*, *85*(3), 454-460.

[7] Park, G., Cudney, H. H., & Inman, D. J. 2000. Impedance-based health monitoring of civil structural components. *Journal of infrastructure systems*, 6(4), 153-160.

[8] Tseng, K. K., & Wang, L. 2004. Smart piezoelectric transducers for in situ health monitoring of concrete. *Smart Materials and Structures*, 13(5), 1017.

[9] Yan, W., & Chen, W. Q. 2010. Structural health monitoring using high-frequency electromechanical impedance signatures. *Advances in Civil Engineering*. 1-11.

[10] Tinoco, H. A., & Marulanda, D. J. 2015. Damage Identification in Active Plates with Indices Based on Gaussian Confidence Ellipses Obtained of the Electromechanical Admittance. *Journal of Nondestructive Evaluation*, *34*(3), 1-16.

[11] Tinoco, H. A., & Marulanda, D. J. 2014. New Index for Damage Identification in Active Beams with Electromechanical Impedance Technique (EMI) Approach to SHM. In: *Proceedings of II International Conference on Advanced Mechatronics, Design, and Manufacturing Technology (AMDM 2014)*. 1-6.

[12] Ribolla, E. L., & Rizzo, P. 2015. Modeling the electromechanical impedance technique for the assessment of dental implant stability. *Journal of biomechanics*, *48*(10), 1713-1720.

[13] Ribolla, E. L. M., Rizzo, P., & Gulizzi, V. 2015. On the use of the electromechanical impedance technique for the assessment of dental implant stability: Modeling and experimentation. *Journal of Intelligent Material Systems and Structures*, *26*(16), 2266-2280.

[14] Moharana, S., Bhalla, S. 2015, Influence of adhesive bond layer on power and energy transduction efficiency of piezo-impedance transducer. *Journal of Intelligent Material Systems and Structure*s; 26(3):247-259.

[15] Tinoco, H.A., & Serpa, A.L. 2012. Voltage relations for debonding detection of piezoelectric sensors with segmented electrode. *Mechanical Systems and Signal Processing*. 31,258-267.

[16] Sirohi, J., & Chopra, I. 2000. Fundamental understanding of piezoelectric strain sensors. *Journal of Intelligent Material Systems and Structures*, 11(4), 246-257.

[17] Liang, C., Sun, F.P., & Rogers, C.A. 1994. Coupled electro-mechanical analysis of adaptive material systems—determination of the actuator power consumption and system energy transfer. *Journal of Intelligent Material Systems and Structures*, 5(1), 12-20.

[18] Tinoco, H.A., & Serpa, A.L. 2011. Bonding influence in the electromechanical (EM) admittance of piezoelectric sensors bonded to structures based on EMI technique. In: Proceedings of the 14th International Symposium on Dynamic Problems of Mechanics (DINAME XIV). Maresias, Brazil 2011; 335-344.

[19] Xu, Y.G., & Liu, G.R. 2012. A modified electro-mechanical impedance model of piezoelectric actuator-sensors for debonding detection of composite patches. *Journal of Intelligent Material Systems and Structures*; 13(6):389-396.

[20] Fu Z.F., & He J. Modal analysis. Butterworth-Heinemann 2001.

[21] Piezoelectric plate: Datasheet of piezoelectric sound components. Sparkfun electronics. 2014. https://www.sparkfun.com/datasheets/Sensors/Flex/p37e.pdf

[22] Analog Devices: Datasheet AD5933. Analog Devices. 2014. http://www.analog.com/static/imported-files/data_sheets/AD5933.pdf

[23] Yan, W., & Chen, W. Q. 2010. Structural health monitoring using high-frequency electromechanical impedance signatures. *Advances in Civil Engineering*. 1-11.

[24] Overly, T.G., Park, G., Farinholt, K.M., & Farrar, CR. 2009 Piezoelectric active-sensor diagnostics and validation using instantaneous baseline data. *Sensors Journal IEEE*, 9(11), 1414-1421.

[25] Hu, X., Zhu, H., & Wang, D. A. 2014. Study of concrete slab damage detection based on the electromechanical impedance method. *Sensors*, 14(10), 19897-19909.

[26] Wang, D., Zhang, J., & Zhu, H. (2015). Embedded Electromechanical Impedance and Strain Sensors for Health Monitoring of a Concrete Bridge.*Shock and Vibration*, *2015*.

[27] Hsu, J. T., Chang, H. W., Huang, H. L., Yu, J. H., Li, Y. F., & Tu, M. G. (2011). Bone density changes around teeth during orthodontic treatment. *Clinical oral investigations*, *15*(4), 511-519.

[28] Chugh, T., Jain, A. K., Jaiswal, R. K., Mehrotra, P., & Mehrotra, R. (2013). Bone density and its importance in orthodontics. *Journal of Oral Biology and Craniofacial Research*, *3*(2), 92-97.

[29] Bridges, T., King, G., & Mohammed, A. (1988). The effect of age on tooth movement and mineraldensity in the alveolar tissues of the rat. *American Journal of Orthodontics and Dentofacial Orthopedics*, *93*(3), 245-250.

[30] Verna, C., Zaffe, D., & Siciliani, G. (1999). Histomorphometric study of bone reactions during orthodontic tooth movement in rats. *Bone*, *24*(4), 371-379.

[31] Melsen, B. (1999). Biological reaction of alveolar bone to orthodontic tooth movement. *The Angle orthodontist*, *69*(2), 151-158.

[32] Verna, C., Dalstra, M., & Melsen, B. (2000). The rate and the type of orthodontic tooth movement is influenced by bone turnover in a rat model.*The European Journal of Orthodontics*, *22*(4), 343-352.

[33] Simmons, D. J., Chang, S. L., Russell, J. E., Grazman, B., Webster, D., & Oloff, C. (1983). The effect of protracted tetracycline treatment on bone growth and maturation. *Clinical orthopaedics and related research*, *180*, 253-259.

[34] Russell, J. E., Grazman, B., & Simmons, D. J. (1984). Mineralization in rat metaphyseal bone exhibits a circadian stage dependency. *Experimental Biology and Medicine*, *176*(4), 342-345.

[35] Cattaneo, P. M., Dalstra, M., & Melsen, B. (2005). The finite element method: a tool to study orthodontic tooth movement. *Journal of dental research*, *84*(5), 428-433.

[36] Cattaneo, P. M., Dalstra, M., & Melsen, B. (2009). Strains in periodontal ligament and alveolar bone associated with orthodontic tooth movement analyzed by finite element. *Orthodontics & craniofacial research*, *12*(2), 120-128.

[37] Liang, W., Rong, Q., Lin, J., & Xu, B. (2009). Torque control of the maxillary incisors in lingual and labial orthodontics: a 3-dimensional finite element analysis. *American Journal of Orthodontics and Dentofacial Orthopedics*,*135*(3), 316-322.

[38] Maki, K., Okano, T., Morohashi, T., Yamada, S., & Shibaski, Y. (1997). The application of three-dimensional quantitative computed tomography to the maxillofacial skeleton. *Dentomaxillofacial radiology*, 26(1), 39-44.

[39] Bhalla, S., & Suresh, R. (2013). Condition monitoring of bones using piezo-transducers. *Meccanica*, 48(9), 2233-2244.

[40] Mazlina, M. H., Sarpinah, B., Tawie, R., Daho, C. D., & Annuar, I. (2016, February). Monitoring of bone healing by piezoelectric- EMI method. In: *Progress in applied mathematics in science and engineering proceedings* (Vol. 1705, p. 020008). AIP Publishing.